

# Double parton scattering via photon-proton interactions: a new light on the transverse proton structure

Matteo Rinaldi

*Dipartimento di Fisica e Geologia. Università degli studi di Perugia,  
INFN section of Perugia. Via A. Pascoli, Perugia, Italy.*

Received 13 January 2022; accepted 18 April 2022

In this contribution we present the main results of the investigation about double parton scattering (DPS) in quasi-real photon-proton interactions. We show the first evaluation of the DPS cross-section at leading-order for the four-jet photo-production observed at HERA. To this aim the  $\gamma - p$  effective cross section has been computed for the first time. One of the main outcomes of this analysis is that the DPS contribution is not negligible and potentially measurable. Furthermore, possible future data could be used to get new information on the transverse proton structure not accessible in other processes.

**Keywords:** Double parton scattering (DPS); quasi-real interactions; photon-proton interactions.

DOI: <https://doi.org/10.31349/SuplRevMexFis.3.0308096>

## 1. Introduction

Here we discuss the main outcomes of Refs. [1]. In collision involving hadrons, the role of multiple parton interactions (MPI), due to extending nature hadrons, has been established [2-9]. Here we focus on double parton scattering (DPS). In fact, new non-perturbative information on the structure of proton, not accessible in single parton scattering (SPS), can be obtained [10-13]. Indeed, the DPS cross-section depends on the almost unknown double Parton Distribution Functions (dPDFs), *i.e.*, the number densities of a parton pair with a given transverse distance  $b_{\perp}$  and carrying longitudinal momentum fractions  $(x_1, x_2)$  of the parent hadron [12-31]. Up today, data on dPDFs are not available and usually, the experimental findings are collected in the so-called  $\sigma_{eff}^{pp}$ , in  $pp$  collisions [32], and recently in  $pA$  collisions [33]. This quantity controls the magnitude of DPS contribution under the assumptions of two uncorrelated hard scatterings and full factorisation of dPDFs in terms of ordinary PDFs. It has been shown that the knowledge of  $\sigma_{eff}^{pp}$  can provide information on the proton structure [10,11]. We remind that from data  $\sigma_{eff} \sim 8 - 35$  mb [34-36]. In Ref. [1] we calculated the DPS cross-section in  $ep$  collisions and thus photon-proton interactions. In fact, the splitting quasi-real photon can initiate the DPS [37]. In particular we considered the four-jet photo-production observed at HERA and analysed by the ZEUS collaboration [38]. In this case, the DPS involves a photon of variable and controllable transverse size, depending on its virtuality  $Q^2$ . Since a complete formulation of photon and proton dPDFs is missing at the moment, we elaborate on a much simpler quantity,  $\sigma_{eff}^{\gamma p}$ . We also include in the analysis the estimate of main background, *i.e.*, the SPS four-jet photo-production cross-section [1]. Furthermore, we then show that the  $Q^2$  dependence of  $\sigma_{eff}^{\gamma p}$  is crucial to obtain the first estimate of the mean transverse distance between partons in the proton. To this aim we provided the necessary integrated lu-

minosity to observe the  $Q^2$  dependence of the DPS cross sections in HERA kinematics.

## 2. Effective cross-section for $\gamma p$ DPS

Here we introduce  $\sigma_{eff}^{\gamma p}$ . One can generalize the definition of the same quantity for  $pp$  collisions [10] which involves the proton effective form factor (eff) [39]. Starting from the proton and photon dPDFs, *i.e.*,  $D_{q_i q_j / p}(x_i, x_j, k_{\perp})$  and  $D_{q\bar{q}/\gamma}(x_k, x_l, k_{\perp})$ , respectively where  $ij$  and  $kl$  are the flavours of the interacting partons,  $k_{\perp}$  is the momentum imbalance, Fourier conjugate variable to the partonic transverse distance,  $b_{\perp}$ , and  $x$ 's are the longitudinal momentum fractions carried by each parton. For both mesons and baryons [13,40-42], dPDFs can be calculated from the Light-Front (LF) wave functions for some quark model. Then, one can define the so called eff [39] which reads, *e.g.*, for the photon:

$$F_2^{\gamma}(\vec{k}_{\perp}) = \frac{\sum_q \int dx D_{q\bar{q}/\gamma}(x, \vec{k}_{\perp}; Q^2)}{\sum_q \int dx D_{q\bar{q}/\gamma}(x, \vec{k}_{\perp} = 0; Q^2)}. \quad (1)$$

This quantity is used to define  $\sigma_{eff}^{\gamma p}$  in the approximation that momentum correlations and parton flavor dependence are neglected. Moreover, if the proton dPDFs can be factorized in terms of PDFs, one gets:

$$\sigma_{eff}^{\gamma p}(Q^2) = \left[ \int \frac{d^2 k_{\perp}}{(2\pi)^2} F_2^p(k_{\perp}) F_2^{\gamma}(k_{\perp}; Q^2) \right]^{-1}. \quad (2)$$

In this scenario, the  $\gamma p$  DPS cross section for the production of the final state  $A + B$  is rearranged in a pocket formula  $\sigma_{DPS}^{A+B} \sim \sigma_{SPS}^A \sigma_{SPS}^B / \sigma_{eff}^{\gamma p}$ . Since there are no data on  $\sigma_{eff}^{\gamma p}(Q^2)$ , in Ref. [1] we calculated it by using the models of Refs. [43,44] to describe both the photon splitting mechanism. For the proton eff, we used the approach of Ref. [20],

which we address as model ‘‘S’’, returning a  $\sigma_{eff}^{pp} \sim 30$  mb. In addition, we also used a Gaussian ansatz. The width of the of this quantity, is a free parameter which produces  $\sigma_{eff}^{pp} = 15$  mb (‘‘G<sub>1</sub>’’ model) and  $\sigma_{eff}^{pp} = 25$  mb (‘‘G<sub>2</sub>’’ model). We remind that in the case of Ref. [44], where the LO QED is used, a detail analysis on the regularization procedure is provided in Ref. [1] We present our numerical estimates for  $\sigma_{eff}^{\gamma p}(Q^2)$  in Fig. 1. One may notice that the hadronic models of Ref. [43] systematically returns a higher  $\sigma_{eff}^{\gamma p}$  with respect to that of Ref. [44]. Moreover, there is large sensitivity to the proton eff. We observe that, in the limit of high photon virtuality, the value of  $\sigma_{eff}^{\gamma p}$  can be predicted in complete analogy with the gluon splitting case elaborated in Ref. [45], see Ref. [1] for details.

### 3. The geometry of $\sigma_{eff}^{\gamma p}(Q^2)$

Here we show how the quantity, previously presented, if measured, could unveil new information on the proton structure. In fact in hadron-hadron collisions, such a goal is almost prevented due to the lack of data on the proton eff [10,11]. Nevertheless, in this case,  $\langle b_{\perp}^2 \rangle_p$ , *i.e.* the main transverse distance between two partons in the proton can be extracted from data on  $\sigma_{eff}^{\gamma p}$ . We consider  $\tilde{F}_2(b_{\perp})$ , probability distribution of finding two partons at a given transverse distance  $b_{\perp}$  [10,11,32], *i.e.*, the Fourier Transform of the eff:

$$\begin{aligned} [\sigma_{eff}^{\gamma p}(Q^2)]^{-1} &= \int d^2 b_{\perp} \tilde{F}_2^p(b_{\perp}) \tilde{F}_2^{\gamma}(b_{\perp}; Q^2) \quad (3) \\ &= \sum_n C_n(\bar{b}_{\perp}; Q^2) \langle (b_{\perp} - \bar{b}_{\perp})^n \rangle_p. \end{aligned}$$

where, in the last passage, we Taylor expanded the photon distribution around  $\bar{b}_{\perp}$ . A realistic description of  $C_n(\bar{b}_{\perp}; Q^2)$ , together with data on the  $Q^2$  dependence of  $\sigma_{eff}^{\gamma p}(Q^2)$ , will allow to access the transverse distance of partons in the proton. In fact, for a given specific dependence of  $C_n$  on  $Q^2$ , one can identify an operator,  $\mathcal{O}_{Q^2}^m$ , such that

$$\mathcal{O}_{Q^2}^m [\sigma_{eff}^{\gamma p}(Q^2)]^{-1} = \mathcal{O}_{Q^2}^m C_m(\bar{b}_{\perp}, Q^2) \langle (b_{\perp} - \bar{b}_{\perp})^m \rangle_p, \quad (4)$$

and then one can select and extract  $\langle (b_{\perp} - \bar{b}_{\perp})^m \rangle_p$ , *i.e.* the relevant information on the proton structure. Details and examples of the application of this procedure are provided in Ref. [1] since data on  $\sigma_{eff}^{\gamma p}$  are not yet available. The only practical limitation is represented by the accuracy with which the dependence of  $\sigma_{eff}^{\gamma p}$  on  $Q^2$  could be eventually measured. This relation strongly motivate this type of measurements at facilities where the photon virtuality can be experimentally measured such as the future Electron Ion Collider [46]. We show here an instructive example.

We consider a Gaussian photon effective form factor and thus the relative normalized probability distribution reads:

$$\tilde{F}_2^{\gamma}(b; Q^2) = \frac{Q^2}{\alpha^2 \pi} e^{-b^2 Q^2 / \alpha^2}. \quad (5)$$

The width depends on a free parameter  $\alpha$ . The main transverse distance between the partons, produced by the splitting mechanism, is:

$$\langle b^2 \rangle_{\gamma} = \int d^2 b b^2 \tilde{F}_2^{\gamma}(b; Q^2) = \frac{\alpha^2}{Q^2}. \quad (6)$$

One should notice that, despite the simplicity of the model, the mean distance between the two produced partons goes to zero, as expected for high virtualities. We can now expand  $\tilde{F}_2^{\gamma}(b; Q^2)$ :

$$\tilde{F}_2^{\gamma}(b; Q^2) \sim \frac{Q^2}{\pi \alpha^2} - \frac{Q^4}{\pi \alpha^4} b^2 + \mathcal{O}(b^4), \quad (7)$$

where  $C_0(Q^2) = Q^2/\pi \alpha^2$  and  $C_2(Q^2) = -Q^4/\pi \alpha^4$ . In this scenario, a suitable operator which isolates  $\langle b^2 \rangle_p$  is  $\hat{\mathcal{O}} = d/(Q^3 dQ)|_{Q^2=0}$ . With this choice, we can prove that:

$$\begin{aligned} \frac{d}{Q^3 dQ} \left( [\sigma_{eff}^{\gamma p}(Q^2)]^{-1} - C_0(Q^2) \right) \Big|_{Q^2=0} &= \quad (8) \\ \frac{d}{Q^3 dQ} \left( C_2(Q^2) \right) \Big|_{Q^2=0} \langle b^2 \rangle_p. \end{aligned}$$

We also consider, for simplicity, that the proton distribution is:

$$\tilde{F}_2^p(b) = e^{-b^2 \beta^2} \frac{\beta^2}{\pi}, \quad (9)$$

and the mean transverse distance reads

$$\int d^2 b b^2 \tilde{F}_2(b) = \frac{1}{\beta^2}. \quad (10)$$

The  $\gamma p$  effective cross section would be:

$$[\sigma_{eff}^{\gamma p}(Q^2)]^{-1} = \frac{\beta^2 Q^2}{\pi(\alpha^2 \beta^2 + Q^2)}, \quad (11)$$

and therefore, the application of the operator leads to:

$$\frac{d}{Q^3 dQ} \left( [\sigma_{eff}^{\gamma p}(Q^2)]^{-1} - C_0(Q^2) \right) \Big|_{Q^2=0} = -\frac{4}{\pi \alpha^4 \beta^2}, \quad (12)$$

$$\frac{d}{Q^3 dQ} \left( C_2(Q^2) \right) \Big|_{Q^2=0} = -\frac{4}{\pi \alpha^4}, \quad (13)$$

which can be combined to give

$$\begin{aligned} \langle b^2 \rangle_p &= \frac{\frac{d}{Q^3 dQ} \left( [\sigma_{eff}^{\gamma p}(Q^2)]^{-1} - C_0(Q^2) \right) \Big|_{Q^2=0}}{\frac{d}{Q^3 dQ} \left( C_2(Q^2) \right) \Big|_{Q^2=0}} \\ &= \frac{1}{\beta^2}, \end{aligned} \quad (14)$$

This is an example of how from the  $Q^2$  dependence of  $\sigma_{eff}^{\gamma p}$  one could extract proton information if the photon splitting mechanism is well established.

#### 4. The four-jet photo-production cross-section

The four-jet photoproduction at HERA has been investigated by the ZEUS collaboration [47] by considering jets with transverse energy  $E_T^{jet} > 6$  GeV and laboratory pseudorapidity  $|\eta_{jet}| < 2.4$ , in the kinematic region  $Q^2 < 1$  GeV<sup>2</sup> and  $y = E_\gamma/E_l$ , *i.e.* the energy fraction transferred between the photon and lepton, in the range  $0.2 \leq y \leq 0.85$ . The collaboration pointed out how the inclusion of MPI significantly improve the description of the data. [38,48,49]. Therefore, in Ref. [1], we adopted the same kinematical cuts of Ref. [47] together with the pocket formula to evaluate  $\sigma_{DPS}$  is now [45]:

$$d\sigma_{DPS}^{4j} = \frac{1}{2} \sum_{ab,cd} \int dy dQ^2 \frac{f_{\gamma/e}(y, Q^2)}{\sigma_{eff}^{\gamma p}(Q^2)} \\ \times \int dx_{p_a} dx_{\gamma_b} f_{a/p}(x_{p_a}) f_{b/\gamma}(x_{\gamma_b}) d\hat{\sigma}_{ab}^{2j}(x_{p_a}, x_{\gamma_b}) \\ \times \int dx_{p_c} dx_{\gamma_d} f_{c/p}(x_{p_c}) f_{d/\gamma}(x_{\gamma_d}) d\hat{\sigma}_{cd}^{2j}(x_{p_c}, x_{\gamma_d}). \quad (15)$$

The sum runs over active parton flavors and  $d\hat{\sigma}^{2j}$  is the differential partonic cross sections. Moreover, we took into account the unintegrated photon flux  $f_{\gamma/e}$  [50] on  $Q^2$  since  $\sigma_{eff}^{\gamma p}$  depends on  $Q^2$ . The distributions  $f_{i/A}(x_{A_i})$  are the proton ( $A = p$ ) and of the photon ( $A = \gamma$ ) PDFs for which we use the leading order sets of Refs. [51,52], respectively. We remark that the Dijet cross sections have been calculated to leading order accuracy by using with ALPGEN [53]. We set both the factorization and renormalization scales to the average transverse momentum of the jets. As discussed in Ref. [1], there are two distinctive contributions determined by the fractional momentum of partons in the photon,  $x_\gamma$ : *i*) the resolved photon, where the photon behaves effectively like an hadron with its own PDF and *ii*) the direct one, where the

photon interacts as a point-like particle. One can notice that the first case populates the whole  $x_\gamma$  range while the latter, at LO, is peaked around at  $x_\gamma = 1$ . Since the two contributions can mix due to higher-order corrections [54], here, as in Ref. [55,56], we considered specific kinematic cuts in order to isolate the resolved mechanism. In the latter case ( $x_\gamma < 0.75$ ) and a direct-enriched one ( $x_\gamma > 0.75$ ). Therefore, we select, in the DPS cross-section,  $x_{\gamma,1} + x_{\gamma,2} < 0.75$ . Furthermore, in order to evaluate the possible background, in Ref. [1], the four-jet photoproduction SPS process has been evaluated to with ALPGEN for  $x_\gamma < 0.75$ , see Table I. Let us address that the experimental four-jet photoproduction cross-section, ( $\sigma_{exp}$ ), turns to be 135 pb for  $x_\gamma < 0.75$  [47]. We report in Table I  $\sigma_{DPS}$  and  $\sigma_{SPS}$  obtained for three ranges of photon virtualities in HERA kinematics. As one can see, the DPS cross section leads to a sizeable non negligible contribution. Moreover, as discussed in Ref. [1], higher order corrections [57-60] for both dijet photo-production and SPS four-jet emission could provide significant effects, see some qualitative details in Ref. [1]. In this case, the LO results could represent: *i*) an upper limit on the SPS background and *ii*) a lower limit on the DPS cross section. Therefore, one should expect that also high order corrections validate the important role of DPS in this process. For the moment being, the largest theoretical uncertainty comes from the models of the proton and photon structures. Nevertheless, a large DPS contribution is predicted by all models adopted, suggesting that jets photoproduction in *ep* collisions could represent a golden channel to observe DPS.

#### 5. Extraction of the $Q^2$ -dependence of $\sigma_{eff}^{\gamma p}$

Here we discuss the  $Q^2$  dependence of the cross-section. The latter is important to extract information on the proton structure. We perform such an analysis within the HERA settings

TABLE I. Predictions for the LO DPS and SPS cross sections for four-jet photo-production in three ranges of  $Q^2$ . In the fourth column, the ratio between the calculated cross-sections to the total one is displayed. In the DPS case, each row corresponds to prediction obtained with a given *pp* eff ( $G_1, G_2, S$ ), and the photon wave function of Refs. [43] (three upper rows) and Ref. [44] (three bottom rows). In the last column the ratio  $R$  is shown.

		$Q^2 \leq 10^{-2}$	$10^{-2} \leq Q^2 \leq 1$	$Q^2 \leq 1$	$\frac{\sigma}{\sigma_{exp}}$	$R$
		[GeV <sup>2</sup> ]	[GeV <sup>2</sup> ]	[GeV <sup>2</sup> ]	[%]	
$\sigma_{DPS}$ [pb]						
w.f.	$G_1$	35.1	18.6	53.7	40	1.89
	$G_2$	29.1	15.2	44.3	33	1.91
[43]	S	26.4	13.7	40.1	30	1.93
w.f.	$G_1$	87.8	54.3	142.1	101	1.62
	$G_2$	54.3	33.4	87.7	65	1.63
[44]	S	50.5	31.1	81.6	60	1.62
$\sigma_{SPS}$ [pb]						
	LO SPS	77.5	36.6	114.1	86	2.12

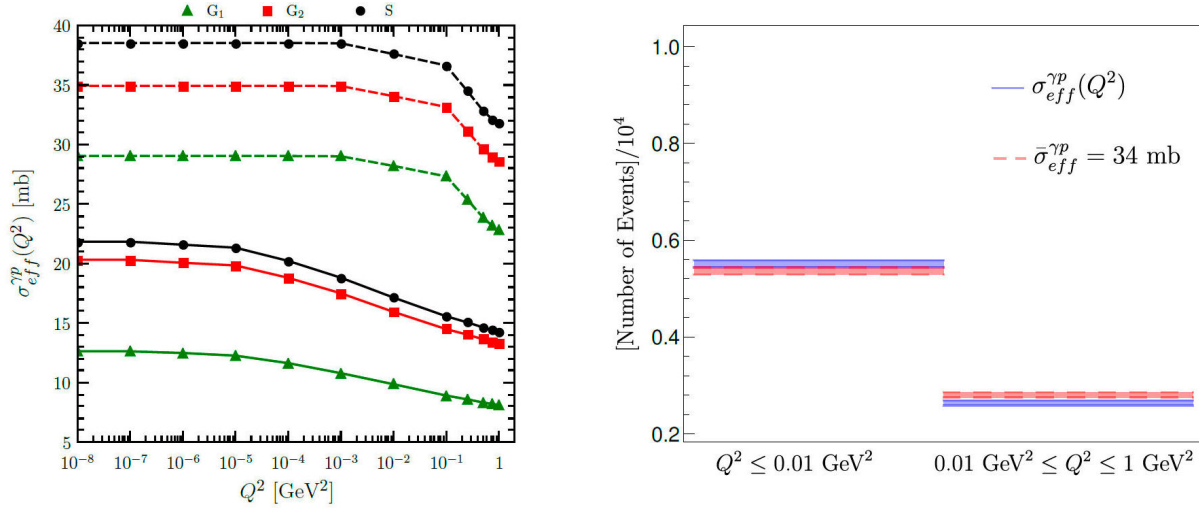


FIGURE 1.  $\sigma_{eff}^{\gamma p}$  evaluated in Eq. (2) with the w.f. of Ref. [43] (dashed lines) and Ref. [44] (full lines) as a function of  $Q^2$ . Different symbols denote the proton effs described in the text. The estimated number of events as a function of  $Q^2$  for  $200 \text{ pb}^{-1}$  of integrated luminosity for the photon model of Ref. [43] and proton eff G2. Full lines stand the evaluations of  $\sigma_{DPS}$  by means of  $\sigma_{eff}^{\gamma p}(Q^2)$  and the dotted ones represent the calculations of  $\sigma_{DPS}$  by using the  $Q^2$ -independent  $\bar{\sigma}_{eff}^{\gamma p}$ .

presented in the previous section. We sketch Eq. (15) as  $d\sigma_{DPS}(bin) \sim \int_{bin} dQ^2 g(Q^2)/\sigma_{eff}^{\gamma p}(Q^2)$ , where  $bin$  stands for a given interval of integration over  $Q^2$  and the function  $g$  encodes the flux factor, the PDFs and elementary cross sections. Then we define the ratio  $R = d\sigma_{DPS}(bin1)/d\sigma_{DPS}(bin2)$ . In the case  $\sigma_{eff}^{\gamma p}$  were a constant, the latter quantity would be:  $R \sim \int_{bin1} dQ^2 g(Q^2)/\int_{bin2} dQ^2 g(Q^2) \sim 2.1$ . Therefore, any discrepancy from this value would directly point to  $Q^2$  effects on  $\sigma_{eff}^{\gamma p}$  or possible correlations breaking the pocket formula. As one can see in the last column of Table I, all models predict a non trivial dependence of  $\sigma_{eff}^{\gamma p}$  on  $Q^2$ . We also estimated the minimum integrated luminosity to experimentally access  $Q^2$  effects in  $\sigma_{eff}^{\gamma p}(Q^2)$ . We have converted the cross sections in Table I in expected number of events with a given integrated luminosity. The results are presented in the right panel of Fig. 1 where we plotted two scenarios: *i*) the blue curves indicate results for the  $\sigma_{eff}^{\gamma p}(Q^2)$ ; *ii*) the red curve indicate the number of events obtained with a constant,  $Q^2$  independent,  $\bar{\sigma}_{eff}^{\gamma p}$  which reproduces the total cross section for  $Q^2 < 1 \text{ GeV}^2$  obtained with  $\sigma_{eff}^{\gamma p}(Q^2)$ . Here we make use of the photon proton models which lead to the the minimal integrated luminosity obtained the two scenarios are distinguished and therefore exposes the  $Q^2$ -dependence of  $\sigma_{eff}^{\gamma p}$  is  $\mathcal{L} = 200 \text{ pb}^{-1}$ . See further details on Ref. [1].

## 6. Conclusions

In the present analysis we have calculated the effective cross sections for photon induced processes which are essential ingredients in the predictions of DPS cross sections in quasi-real photon proton interactions. The latter have been evaluated by means of electromagnetic and hadronic models of the photon and proton structures, respectively. For the four-jet final state in HERA kinematics we found a sizeable DPS contribution.

In the case the photon virtuality  $Q^2$  could be measured, we have proven that data on  $\sigma_{eff}^{\gamma p}$  could be used to extract new information on the proton structure. We set lower limits on the integrated luminosity needed to observe such a dependence.

## Acknowledgements

This work was supported, in part by the STRONG-2020 project of the European Unions Horizon 2020 research and innovation programme under grant agreement No 824093 and by the project ‘‘Photon initiated double parton scattering: illuminating the proton parton structure’’ on the FRB of the University of Perugia. The author thank the organizers of the ‘‘19th International Conference on Hadron Spectroscopy and Structure (HADRON2021)’’.

1. M. Rinaldi and F. Alberto Ceccopieri, Enlightening the transverse structure of the proton via double parton scattering in photon-induced interactions. *Phys. Rev. D* **3** (2021)
2. C. Goebel, F. Halzen, and D. M. Scott, Double Drell-Yan Anihilations in Hadron Collisions Novel Tests of the Constituent

Picture. *Phys. Rev. D*, **22** (1980) 2789.

3. B. Humpert, ARE THERE MULTI - QUARK INTERACTIONS? *Phys. Lett. B*, **131** 461-467 (1983)
4. M. Mekhfi, MULTIPARTON PROCESSES AN APPLICA-

- TION TO DOUBLE DRELL-YAN. *Phys. Rev. D*, **32** (1985) 2371.
5. M. Mekhfi, Correlations in Color and Spin in Multiparton Processes. *Phys. Rev. D*, **32** (1985) 2380.
  6. B. Humpert and R. Odorico., Multiparton Scattering and QCD Radiation as Sources of Four Jet Events. *Phys. Lett. B*, **154** (1985) 211.
  7. M. L. Mangano, Four Jet Production at the Tevatron Collider. *Z. Phys. C*, **42** (1989) 331.
  8. N. Paver and D. Treleani, Multi - Quark Scattering and Large pT Jet Production in Hadronic Collisions. *Nuovo Cim. A*, **70** (1982) 215.
  9. T. Sjostrand and M. van Zijl, Multiple Parton-parton Interactions in an Impact Parameter Picture. *Phys. Lett. B* **188** (1987) 149-154.
  10. M. Rinaldi and F. Alberto Ceccopieri, Hadronic structure from double parton scattering. *Phys. Rev. D* **97** (2018) 071501.
  11. M. Rinaldi and F. A. Ceccopieri, Double parton scattering and the proton transverse structure at the LHC. *JHEP*, **09** (2019) 097.
  12. M. Rinaldi, S. Scopetta, M. Claudio Traini, and V. Vento, Correlations in Double Parton Distributions Perturbative and Non-Perturbative effects. *JHEP*, **10** (2016) 063.
  13. M. Rinaldi, S. Scopetta, M. Traini, and V. Vento, Double parton correlations and constituent quark models a Light Front approach to the valence sector. *JHEP*, **12** (2014) 028.
  14. M. Diehl, D. Ostermeier, and A. Schafer, Elements of a theory for multiparton interactions in QCD. *JHEP*, **03** (2012) 089. [Erratum JHEP03,001(2016)].
  15. M. Diehl and A. Schafer, Theoretical considerations on multiparton interactions in QCD. *Phys. Lett. B* **698** (2011) 389-402.
  16. Aneesh V. Manohar and Wouter J. Waalewijn, A QCD Analysis of Double Parton Scattering Color Correlations, Interference Effects and Evolution. *Phys. Rev.*, **85** (2012) 114009.
  17. M. Rinaldi, S. Scopetta, and V. Vento, Double parton correlations in constituent quark models. *Phys. Rev. D* **87** (2013) 114021.
  18. B. Blok, Yu. Dokshitzer, L. Frankfurt, and M. Strikman, pQCD physics of multiparton interactions. *Eur. Phys. J. C* **72** (2012) 1963.
  19. B. Blok, Yu. Dokshitzer, L. Frankfurt, and M. Strikman, The Four jet production at LHC and Tevatron in QCD. *Phys. Rev. D* **83** (2011) 071501.
  20. B. Blok, Yu. Dokshitzer, L. Frankfurt, and M. Strikman, Perturbative QCD correlations in multi-parton collisions. *Eur. Phys. J. C* **74** (2014) 2926.
  21. J. R. Gaunt and W. James Stirling, Double Parton Distributions Incorporating Perturbative QCD Evolution and Momentum and Quark Number Sum Rules. *JHEP*, (2010) 005.
  22. H.-M. Chang, A. V. Manohar, and W. J. Waalewijn, Double Parton Correlations in the Bag Model. *Phys. Rev. D* **87** (2013) 034009.
  23. M. Diehl, J. R. Gaunt, D. M. Lang, P. Pläbfl, and A. Schäfer, Sum rule improved double parton distributions in position space. *Eur. Phys. J. C* **80** (2020) 468.
  24. M. Diehl, P. Pläbfl, and A. Schäfer, Proof of sum rules for double parton distributions in QCD. *Eur. Phys. J. C*, **79** (2019) 253.
  25. M. Diehl, J. R. Gaunt, and K. Schönwald, Double hard scattering without double counting. *JHEP*, **06** (2017) 083.
  26. M. Diehl, J. R. Gaunt, D. Ostermeier, P. Pläbfl, and A. Schäfer, Cancellation of Glauber gluon exchange in the double Drell-Yan process. *JHEP*, **01** (2016) 076.
  27. J. R. Gaunt, Glauber Gluons and Multiple Parton Interactions. *JHEP*, **07** (2014) 110
  28. M. Diehl, J. R. Gaunt, P. Pläbfl, and A. Schäfer, Two-loop splitting in double parton distributions. *SciPost Phys.*, **7** (2019) 017.
  29. M. Diehl and R. Nagar, Factorisation of soft gluons in multiparton scattering. *JHEP*, **04** (2019) 124.
  30. M. G. Ryskin and A. M. Snigirev, A Fresh look at double parton scattering. *Phys. Rev. D* **83** (2011) 114047.
  31. M. G. Ryskin and A. M. Snigirev, Double parton scattering in double logarithm approximation of perturbative QCD. *Phys. Rev. D* **86** (2012) 014018.
  32. G. Calucci and D. Treleani, Proton structure in transverse space and the effective cross-section. *Phys. Rev. D* **60** (1999) 054023.
  33. R. Aaij *et al.*, Observation of Enhanced Double Parton Scattering in Proton-Lead Collisions at psNN =8.16 TeV. *Phys. Rev. Lett.*, **125** (2020) 212001.
  34. M. Aaboud *et al.*, Study of hard double-parton scattering in four-jet events in pp collisions at ps = 7 TeV with the ATLAS experiment. *JHEP*, **11** (2016) 110.
  35. CMS. Study of double-parton scattering in the inclusive production of four jets with low transverse momentum in proton-proton collisions at ps = 13 TeV. CMS-PAS-SMP-20-007 (2021)
  36. E. Chapon *et al.*, Perspectives for quarkonium studies at the high-luminosity LHC. (2020)
  37. M. Klasen, Theory of hard photoproduction. *Rev. Mod. Phys.*, **74** (2002) 1221-1282.
  38. J. M. Butterworth, J. R. Forshaw, and M. H. Seymour, Multiparton interactions in photoproduction at HERA. *Z. Phys. C*, **72** (1996) 637-646.
  39. M. Rinaldi, S. Scopetta, M. Traini, and V. Vento, Double parton scattering a study of the effective cross section within a Light-Front quark model. *Phys. Lett. B* **752** (2016) 40-45.
  40. M. Rinaldi, S. Scopetta, M. Traini, and V. Vento, A model calculation of double parton distribution functions of the pion. *Eur. Phys. J. C* **78** (2018) 781.
  41. T. Kasemets and A. Mukherjee, Quark-gluon double parton distributions in the light-front dressed quark model. *Phys. Rev. D* **94** (2016) 074029.
  42. M. Rinaldi, Double parton correlations in mesons within AdS/QCD soft-wall models a first comparison with lattice data. *Eur. Phys. J. C* **80** (2020) 678.
  43. A. E. Dorokhov, W. Broniowski, and E. Ruiz Arriola, Photon distribution amplitudes and light-cone wave functions in chiral quark models. *Phys. Rev. D* **74** (2006) 054023.

44. S. J. Brodsky, L. Frankfurt, J. F. Gunion, A. H. Mueller, and M. Strikman. Diffractive lepton production of vector mesons in QCD. *Phys. Rev. D* **50** (1994) 3134-3144.
45. J. R. Gaunt, Single Perturbative Splitting Diagrams in Double Parton Scattering. *JHEP*, **01** (2013) 042.
46. R. Abdul Khalek *et al.*, Science Requirements and Detector Concepts for the Electron-Ion Collider EIC Yellow Report. (2021)
47. S. Chekanov *et al.*, Three- and four-jet final states in photoproduction at HERA. *Nucl. Phys. B*, **792** (2008) 1-47.
48. G. Marchesini, B. R. Webber, G. Abbiendi, I. G. Knowles, M. H. Seymour, and L. Stanco, HERWIG A Monte Carlo event generator for simulating hadron emission reactions with interfering gluons. Version 5.1 - April 1991. *Comput. Phys. Commun.*, **67** (1992) 465-508.
49. T. Sjostrand *et al.*, High-energy physics event generation with PYTHIA 6.1. *Comput. Phys. Commun.*, **135** (2001) 238-259.
50. S. Frixione, M. L. Mangano, P. Nason, and G. Ridolfi, Improving the Weizsacker-Williams approximation in electron - proton collisions. *Phys. Lett. B*, **319** (1993) 339-345.
51. J. Pumplin *et al.*, New generation of parton distributions with uncertainties from global QCD analysis. *JHEP* **07** (2002) 012.
52. M. Gluck, E. Reya, and A. Vogt. Photonic parton distributions. *Phys. Rev. D* **46** (1992) 1973-1979
53. M. L. Mangano, M. Moretti, F. Piccinini, R. Pittau, and A. D. Polosa, ALPGEN, a generator for hard multiparton processes in hadronic collisions. *JHEP*, **07** (2003) 001.
54. S. Frixione and G. Ridolfi, Jet photoproduction at HERA. *Nucl. Phys. B*, **507** (1997) 315-333.
55. S. Chekanov *et al.*, High-E(T) dijet photoproduction at HERA. *Phys. Rev. D*, **76** (2007) 072011.
56. A. Aktas *et al.*, Photoproduction of dijets with high transverse momenta at HERA. *Phys. Lett. B*, **639** (2006) 21-31.
57. M. Klasen and G. Kramer, Inclusive two jet production at HERA Direct and resolved cross-sections in next-to-leading order QCD. *Z. Phys. C*, **76** (1997) 67-74.
58. M. Klasen, T. Kleinwort, and G. Kramer, Inclusive Jet Production in p and Processes Direct and Resolved Photon Cross Sections in Next-To-Leading Order QCD. *Eur. Phys. J. direct*, **1** (1998) 1.
59. S. Badger, B. Biedermann, P. Uwer, and V. Yundin, NLO QCD corrections to multi-jet production at the LHC with a centre-of-mass energy of  $\sqrt{s} = 8$  TeV. *Phys. Lett. B*, **718** (2013) 965-978.
60. Z. Bern *et al.*, Four-Jet Production at the Large Hadron Collider at Next-to-Leading Order in QCD. *Phys. Rev. Lett.*, **109** (2012) 042001.